CONF-9507170--1

LA-UR-. 95-3126

Title: RESIDUAL STRESS AND MICROSTRUCTURAL CHARACTERIZATION USING RIETVELD REFINEMENTS OF A CARBURIZED LAYER IN A 5120 STEEL

Author(s): P. Rangaswamy, M. A. M. Bourke, A. C. Lawson, J. O'Rourke, J. A. Goldstone

Submitted to: Advances in X-Ray Analysis

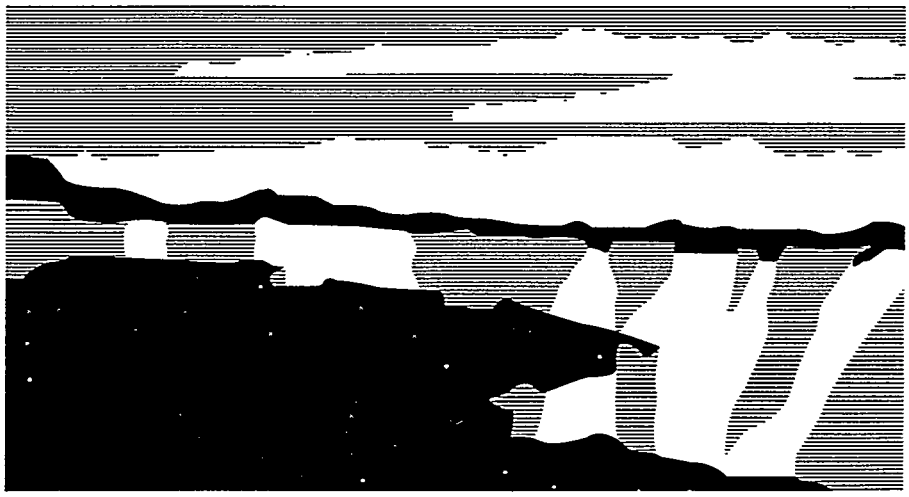

Residual Stress and microstructural characterization using Rietveld refinement of a carburized layer in a 5120 steel

P. Rangaswamy, M. A.M. Bourke, A. C. Lawson, J. O' Rourke, & J. A. Goldstone

Los Alamos National Laboratory, Los Alamos, NM, 87545, USA

Rietveld refinement of X-ray diffraction patterns has been used to provide microstructural information complementary to conventional X-ray residual stress measurements through a carburized layer containing a maximum vol. 25 % of retained austenite. Layers in a simple specimen were removed incrementally by electropolishing and, at each depth in addition to conventional residual stress measurements in both the martensite and retained austenite, data were collected at $\psi = 0$ for Rietveld refinement. The refinements provide accurate values for the lattice parameters in the respective phases that can be related to carbon content and microstructure. Besides to providing qualitative information concerning the microstructure and possible surface decarburization, the c/a ratio of the martensite potentially offers an independent technique for determining carbon content profiles.

1. INTRODUCTION.

Carburization is widely applied to steel components to harden the surface, thereby improving wear and fatigue resistance. Its microstructural implications are well understood and there is considerable literature describing its implications [1-6]. However, it is inevitably associated with distortions that impede the manufacturing cycle by compromising tolerances and are difficult to predict, requiring trial and error approaches to identify suitable heat treat conditions for new parts. Although the distortion and precursor residual stresses resulting from heat treatments have been widely studied, accurate predictions for new geometries remain elusive. Consequently, accurate profiling of residual stress and microstructures resulting from carburization remains a focus for study.

During carburization, carbon diffuses into the surface, changing the composition (over a distance of typically about 1 mm below the surface), with the highest carbon content usually at the surface. The region of elevated carbon content, called the case, has a lower martensite start transformation temperature (M_s) with respect to the interior. For small parts during quenching, there is little lag time between the temperatures at the surface and the interior. Consequently, during quenching from the austenitizing temperature of ≈1550°F

the interior transforms first, then the subsequent transformation and dilation of the surface austenite is resisted by hard underlying martensite. The result is an in-plane compressive macrostress that is a maximum at or close to, the surface and is similar in shape to that produced by shot peening. The shape of the profile depends on the carburization conditions, the amount of retained austenite, and the subsequent tempering.

In this work, complementary depth profiles of residual stress and microstructure were recorded and analyzed through a carburized layer (containing a significant volume fraction of retained austenite) using X-ray diffraction techniques and the Rietveld method [7]. The case contains steep stress and microstructure gradients. Since X-ray penetration is small compared to the case X-ray diffraction is an accepted practice for profiling residual stresses. By electropolishing, successive layers are removed exposing layers deeper into the material. One issue of paramount importance to the accurate prediction of distortion is the carbon profile. This is usually measured independently using burn-up or microprobe methods or by inference from hardness measurements but the lattice parameters of both austenite and martensite provide an independent source for the carbon profiles [8,9]. By using the Rietveld technique to document changes in lattice parameters at the same time as stress measurements are performed, the carbon content can also be identified with little extra effort.

2. SPECIMENS

Multiple cylindrical pucks (diameter 30 mm and thickness 10 mm were cut from 5120 bar stock having a composition detailed in table 1. One flat surface of each puck was polished, and all the profiles were performed through this surface. The pucks were carburized for 35 hours at 1650° F at a carbon potential of 0.8, quenched and tempered.

TABLE 1

Composition of 5120 bar stock prior to carburization

Element	C	Mn	P	S	Si	Ni	Cr	Mo	Cu	Al	N	O
Wt %	.23	.83	.012	.025	.22	.15	.8	.04	.15	.031	.008	.003

3. X-RAY DIFFRACTION MEASUREMENTS.

Stress measurements were performed using standard methodology as outlined in SAE-J784A [10,11] with a Phillips vertical diffractometer operating at 40KV and 10mA. The spot was 2 mm in diameter. All measurements used Cr radiation (wavelength ≈ 2.289Å) for which the martensitic (211) reflection appears at ≈ 156° (2θ) and the austenite (220)

reflection at ≈ 128° (2θ). At the surface the martensitic reflection was ≈14° wide with 85% of the intensity coming from a width of 4° (2θ). At $\psi = 0°$ the penetration depth is ≈ 5.5 microns and at $\psi = 60°$ is ≈ 3 microns. A circular region 6 mm in diameter was electropolished at the center of the puck using a mixture of phosphoric and sulfuric acids with distilled water (at 54°C), in the ratio of 2 : 1 : 1 by volume. The current was controlled at an approximate current density of 0.0042 A/mm^2 chosen to minimize surface pitting. Measured intensities were corrected for absorption at different ψ tilts, and normalized with respect to the Lorentz-Polarization factors. Background corrections were applied before calculating peak positions using the conventional parabolic technique.

Stresses in both martensite and austenite phases were calculated (using an x-ray elastic constant of 6.3 x 10^{-6} MPa^{-1}) in two orthogonal directions at the center of the puck. Both positive and negative ψ tilts were recorded (splitting was not observed). The raw stresses are shown in Figures 2 (a & b). Layer removal corrections were performed using the procedure outlined by Moore and Evans [12] which assumes that a complete layer is removed in each step and the corrected martensitic stresses are shown in Figures 3. Stresses were recorded to a maximum depth of 1.2 mm. Austenite volume fractions were also determined using the conventional technique comparing intensities of the austenite (220) and martensitic (200 002) reflections (Figure 4).

At each depth θ/2θ scans from 40 to 162° 2θ were recorded at $\psi = 0$ for Rietveld structure refinements using GSAS [13]. By assuming a body centered tetragonal structure (I4/mmm) for the martensite and, where appropriate close to the surface, a face centered cubic structure (Fm3m) for the retained austenite, predicted peak positions and intensities were matched to measured diffraction patterns. In addition to the lattice parameters, phase ratios, strain broadening terms were determined. Refinements for the surface and for a 1 mm depth are included in figures 5 (a,b). The tick marks indicate the positions of the peaks (including $K_{\alpha 1}$ and $K_{\alpha 2}$) and the difference between predicted and observed intensities is shown below. For the data at 1 mm depth, the austenite reflections are absent while the martensite reflections are sharper and displaced compared to the martensite reflections on the surface. Changes in a_o for austenite over the first 400 microns are include in Figure 6, and the martensitic lattice parameters and their ratio are shown in Figures 7 and 8.

4. DISCUSSION

For this heat treament the results in figure 2 and 3 indicate that the maximum compressive stress of - 455 MPa is about 600 microns from the surface and rises quite sharply towards

tensile stresses. Over the first 200 microns from the surface, the stresses show considerable scatter but thereafter the profiles are smoother. The distribution of the stresses is consistent with published data [1-2,4,6,15]. Retained austenite measurements using the conventional and Rietveld refinement technique are presented in Figure 4. Austenite composition varies from 20 vol% at the surface to a maximum of 30% at 50 microns thereafter decreasing to less than 5% at about 600 microns depth. In the conventional approach, austenite volume fraction is determined by comparing integrated intensities from only two peaks whereas the Rietveld techniques calculates phase fractions using a least square's minimization of an entire powder pattern (which admittedly in this case only consists of 3 peaks of each phase). The trends between conventional and Rietveld determinations are similar except for differences in magnitude not exceeding 5%. By analogy with the improved accuracy associated with the four-peak method [14] it is possible that Rietveld refinement is better still since it uses data from the entire pattern.

Comparison of the stress and austenite data indicates that the maximum compressive stress occurs at a depth comparable to that at which the austenite volume fraction reaches a minimum. An additional observation is that the lattice parameters for the two phases show a marked reduction associated with the first 100μm. This appears to correlate with the region of reduced austenite , and preliminary metallography suggests that this may be a decarburized layer. In fact, the combined assessment suggests that the carbon profile as interpreted in the austenite and martensite phases is not a maximum at the surface (see next paragraph) and that the martensitic stress has an intermediate minimum below the surface.

Since the relationship between lattice parameter of both the austenite and martensite can be directly related to carbon content, their changes can be used to infer the carbon profiles. Of course these changes are also affected by stress but the relative magnitude of the effects supports the assumption that the dominant part of the shifts noted in figures 6 and 7 is due to distortion of the respective lattices by varying C content. This is supported by the fact that the scans were performed at $\psi = 0$, i.e. the scattering vector was normal to the surface. Nevertheless it could be argued that the contribution from the elastic strain normal to the surface is difficult to quantify accordingly we focused on the martensitic lattice parameters. Since these include a "c" and an "a" lattice parameter which change in opposing senses with C content, this provides us a mechanism to decouple the stress complication.

For the material through the case the lattice parameter dependence on carbon content was determined by independent neutron measurements, performed at IPNS using the GPPD

spectrometer, on direct quench specimens of 5120, 5140, 5160 and 5180 steels which have uniform carbon contents of 0.2, 0.4, 0.6 and 0.8 wt%. These compositions span the range expected through the case. Lattice parameters were determined using the Rietveld method as a function of carbon content. The c/a ratio can be related to carbon content in the above calibration specimens then that relationship is used to infer a carbon profile from the results in figure 8. The carbon content calculated using this method is overlaid with the results of combustion analysis on a sample identically heat-treated in figure 9. Below 350μm there is excellent agreement between the two determinations but closer to the surface the agreement is only qualitative. Further conclusions require metallography to establish whether only martensite and austenite are present - since the presence of carbides (although unlikely) would invalidate the comparisons since the burn up is a bulk technique while in the diffraction approaches carbides are not accounted for .

5 CONCLUSIONS

We have successfully shown that Rietveld analysis holds promise in characterizing the microstructure and potentially aids in the interpretation of stress measurements. Collection of the data necessary for a Rietveld refinement can easily be performed during electropolishing measurements for stress. These results offer an independent method indicative of decarburization as well as offering a viable method for determining carbon profiles.

Other specific conclusions are:

1. Maximum compression occurs 600 microns below surface.
2. Using a Moore & Evans correction the crossover from compression to tension is between 1 and 1.2 mm below surface.
3. Austenite volume fraction ~ 25% at surface increasing slightly to a maximum of 30% at ~100 microns and subsequently falls to ~ 5% at a depth of 600 microns.
4. Martensite and austenite stresses in first 250 microns are not statistically different.
5. Maximum compressive stress corresponds to the position at which retained austenite volume fraction reaches a minimum of ~ 5% .

ACKNOWLEDGMENTS

This work was pursued as part of a DOE CRADA (#?) in collaboration with industry participants through the national center for manufacturing sciences. We gratefully acknowledge Maurice Howes and Gerry Koller from IITRI for heat treating the specimens.

We also acknowledge the use of Intense Pulsed Neutron Source operated as a national user facility by the United States Department of Energy, Basic Engineering Sciences - Material Sciences, under contract No. W-31-109-ENG-38.

REFERENCES

1. Heat Treatment, Microstructures, and Residual Stresses in Carburized Steels, G. Krauss, Proceedings of the First Conference on Quenching & Control of Distortion, Chicago, Illinois, USA, 22-25 September 1992.
2. D. P. Koistinen, Trans. ASM, 1958, 50, 227.
3. Modeling Distortion and Residual Stress in Carburized Steels, M. Henriksen, D.B. Larson, and C. J. Van Tyne, Proceedings of the First Conference on Quenching & Control of Distortion, Chicago, Illinois, USA, 22-25 September 1992.
4. L. J. Ebert, Metallurgical Transactions A, Volume 9A, Nov 1978 (1537-1551)
5. R.C. Fischer, Metallurgical Transactions A, Volume 9A, Nov 1978 (1553-1560)
6. G. Krauss, Metallurgical Transactions A, Volume 9A, Nov 1978 (1527-1535)
7. R.B., Von Dreele, J.D. Jorgensen, & C.G.Windsor Journal of Applied Crystallography, 15, 581-589.1982
8. C. S. Robert, "Effect of Carbon on the Volume Fractions and Lattice parameters of Retained Austenite and Martensite", Trans. AIME, Journal of Metals, Feb, 1953, Pp 203-204.
9. Zenji Nishiyama, "Martensitic Transformation', 1978, Pp 14 - 20.
10. "Residual Stress Measurement by X-ray Diffraction", SAE Information Report J784a, M.E. Hilley, Ed., Society of Automotive Engineers, New York, August 1971.
11. Residual Stress, Measurement by Diffraction and Interpretation, I.C. Noyan and J. B. Cohen, Eds., Springer-Verlag, New York, (1987)
12. "Mathematical correction for stress in removed layers in X-ray diffraction residual stress analysis", M.G. Moore, W.P. Evans, SAE Transactions, p341 Vol66 1958.
13. A. C. Lawson and R. B. Von Dreele, Generalized crystal structural analysis system, LAUR 86-748, 1966 (Los Alamos National Laboratory)
14. B. Pardue and L. Lowery, "Four-Peak Retained Austenite Analysis using X-ray diffraction (XRD), Adv. X-ray Analysis, 43, (1994) - in publication.
15. Chongmin Kim, Adv. X-ray Analysis, 25, 1981, Pp 343-

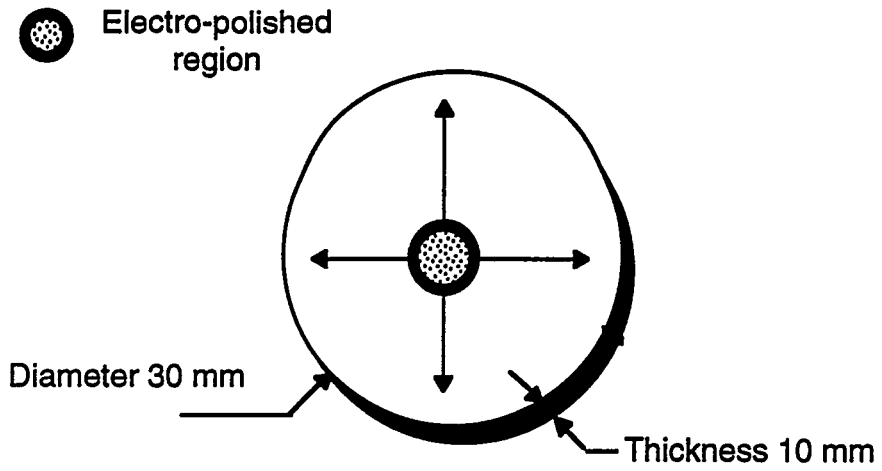

Figure 1. Schematic drawing of the Carburized Puck showing the measurement location and directions.

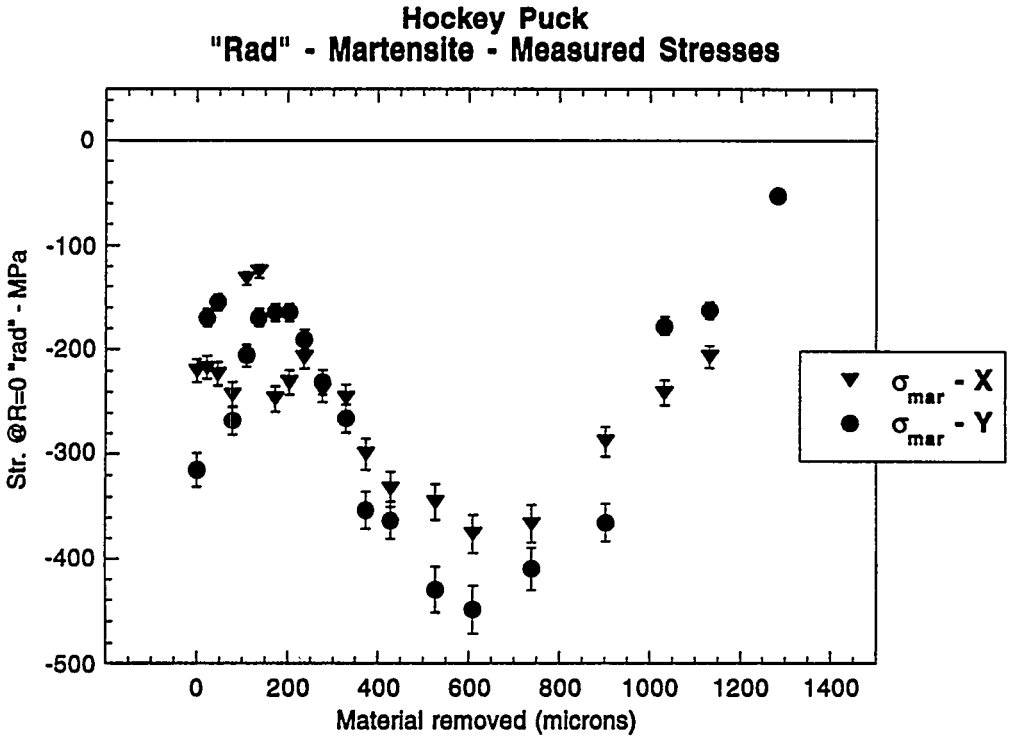

Figure 2 a. Residual stress profile in the martensitic phase (Un-corrected)

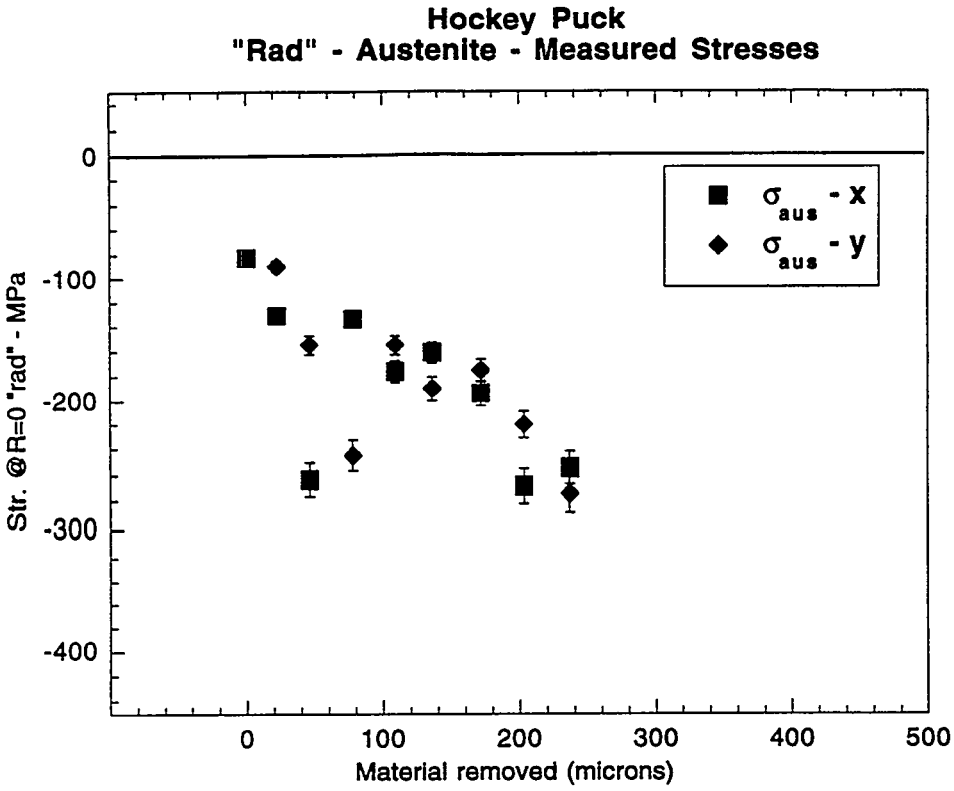

Figure 2 b. Residual stress profile in the austenite phase (Un-corrected)

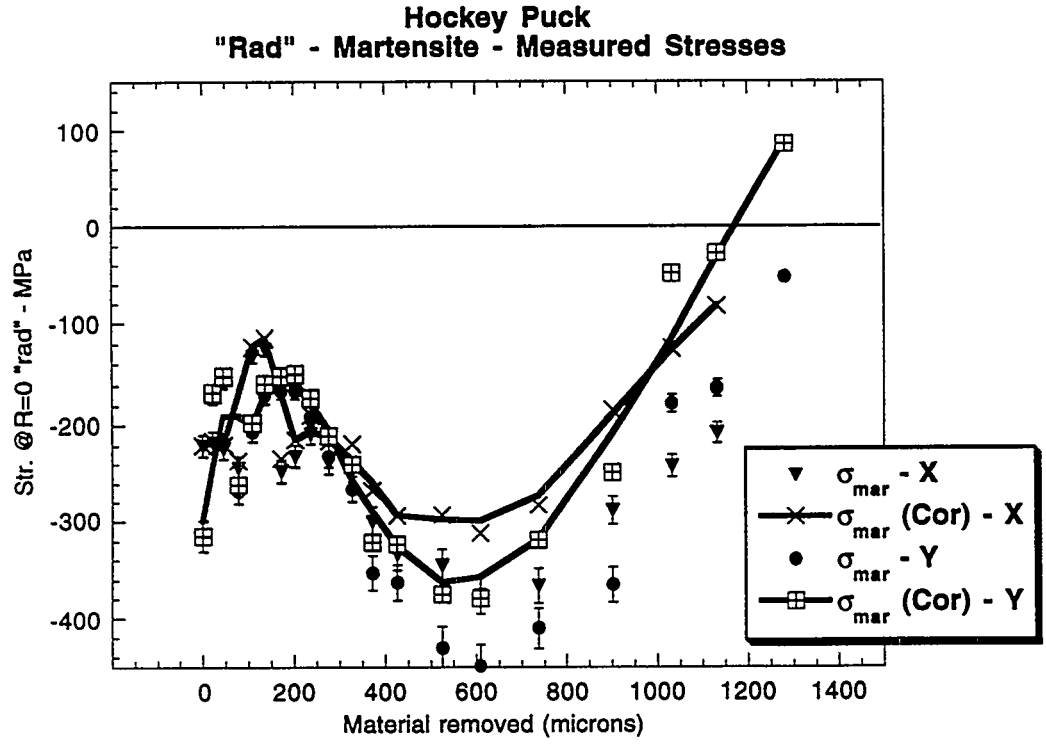

Figure 3. Residual stress profile in the martensitic phase (corrected)

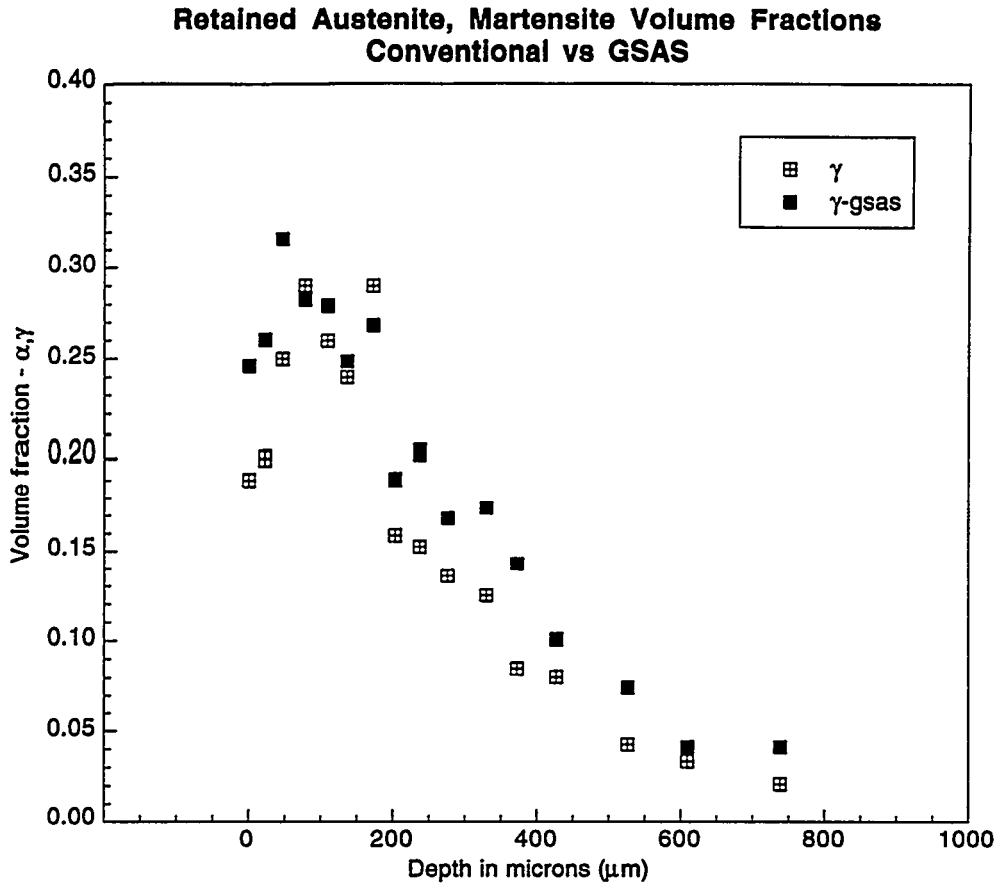

Figure 4. Retained austenite profiles using conventional and GSAS.

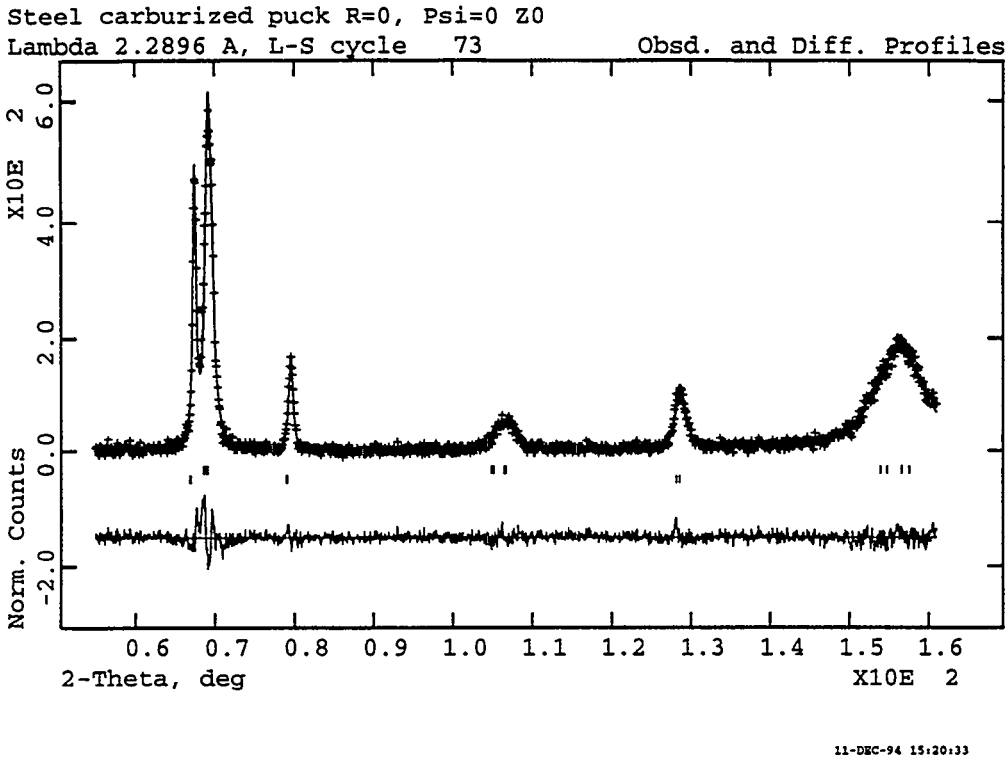

Figure 5a. Reitveld refinements for the surface showing both austenite and martensitic reflections.

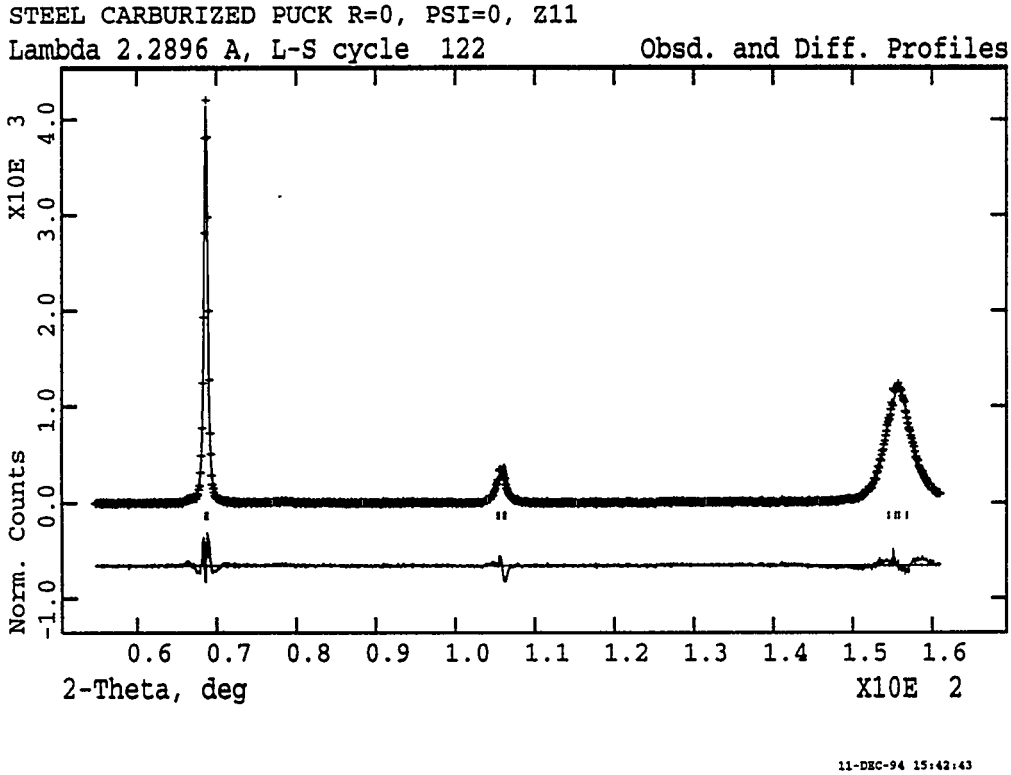

Figure 5b. Reitveld refinements at 1 mm depth below the surface showing martensitic reflections only.

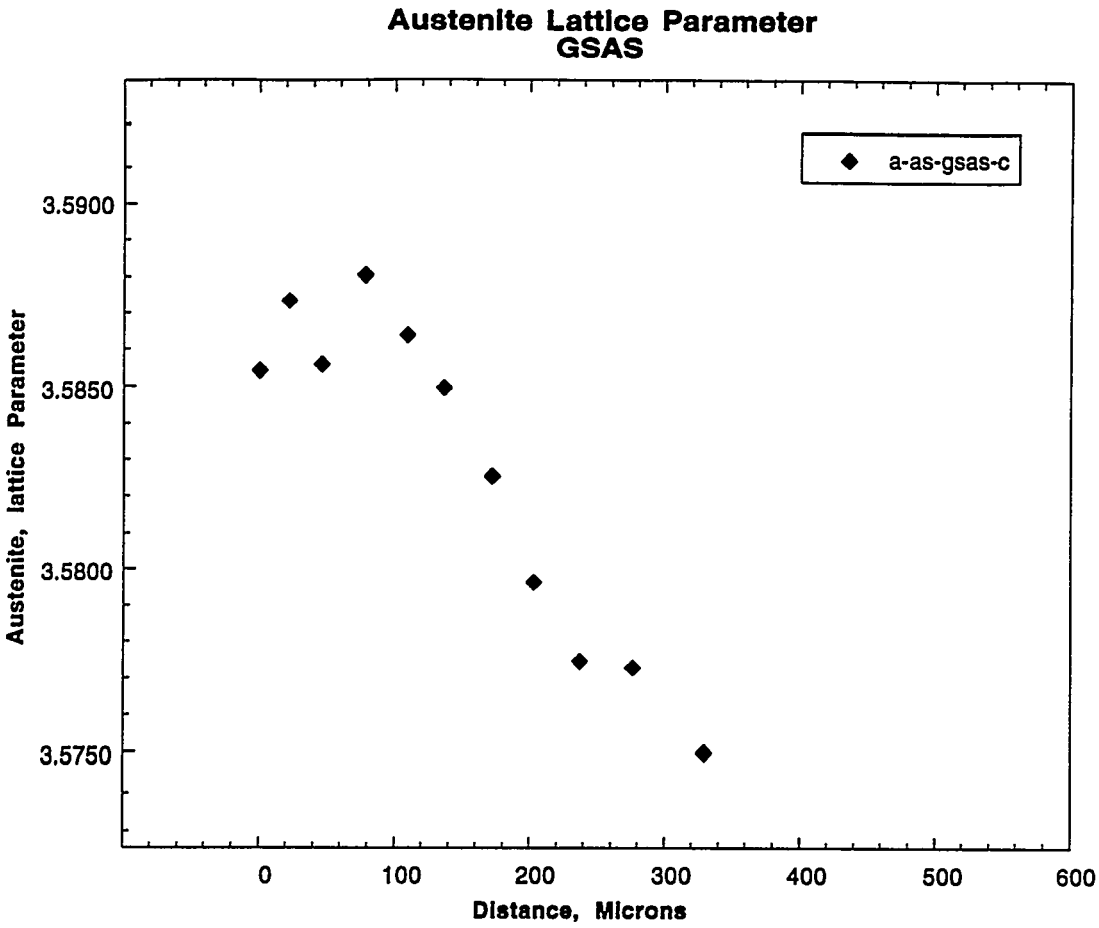

Figure 6. Profile of lattice parameters for austenite.

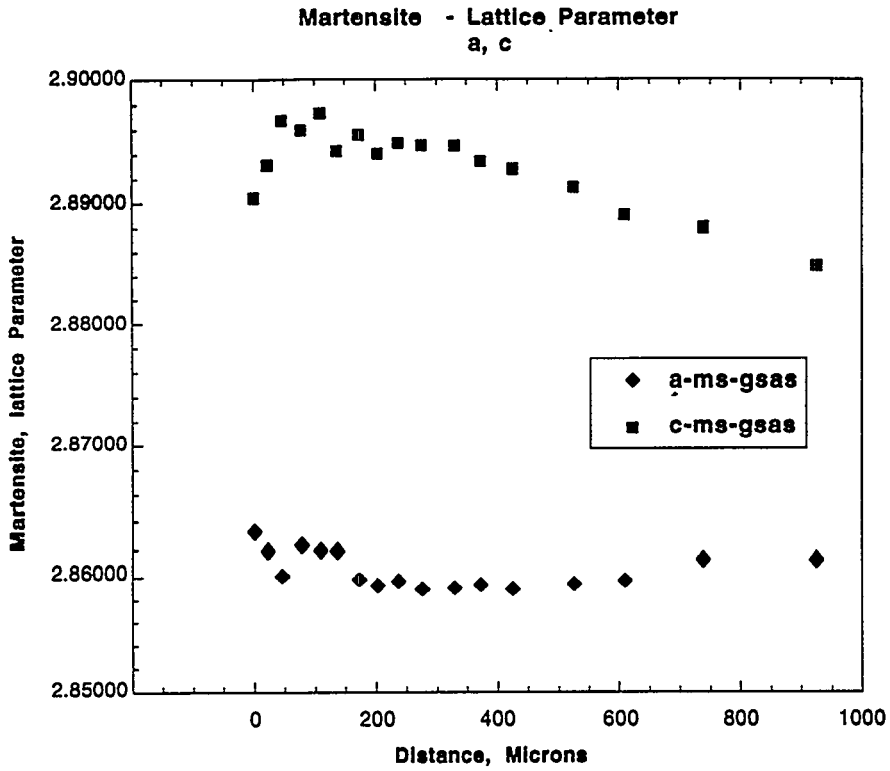

Figure 7. Profile of lattice parameters for martensite.

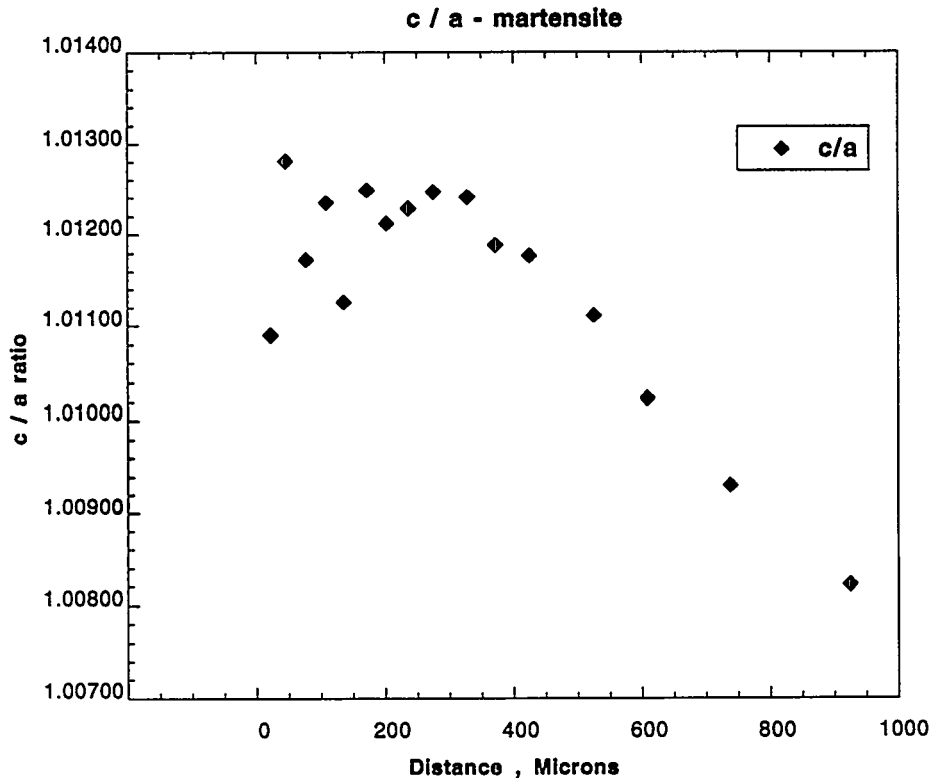

Figure 8. Profile of c/a ratio of martensite lattice parameters.

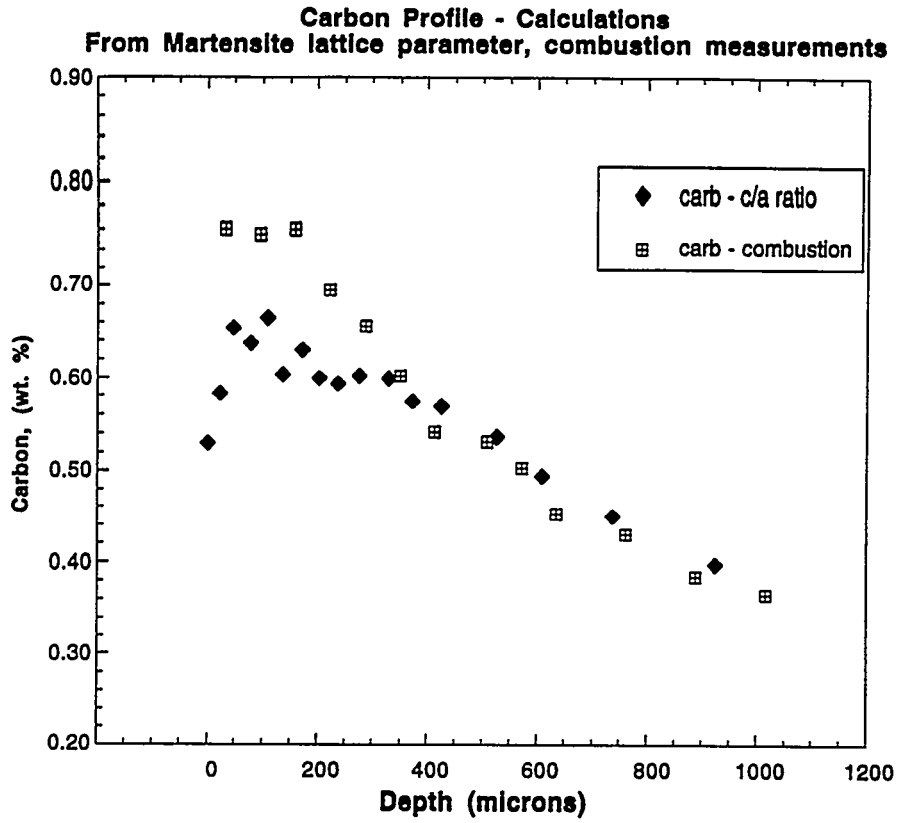

Figure 9. Comparison of carbon profiles calculated from c/a ratio and independent measurements using combustion techniques.